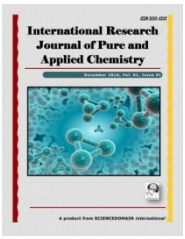

International Research Journal of Pure & Applied Chemistry
4(5): 541-550, 2014

SCIENCEDOMAIN *international*
www.sciencedomain.org

Support Material Effect for Pt Catalytic Activity at Cathode

Rikson Siburian[1*]

[1]*Department of Chemistry, Faculty of Science and Engineering, University Of Nusa Cendana, Kupang, East of Nusa Tenggara, Indonesia.*

Author's contribution

This whole work was carried out by the author RS.

Original Research Article

Received 20th February 2014
Accepted 24th April 2014
Published 15th May 2014

ABSTRACT

The graphene nano sheets (GNS) and nitrogen doped graphene (N-G) were used as supporting materials to deposit Pt particles in order to investigate the support material effect for oxygen reduction reaction (ORR) activity. The ORR activity of platinum on GNS (Pt/GNS) is higher than Pt/N-G catalysts. This suggests that the modification of π states by the N-doping change the properties of the interaction between Pt and carbon. The interaction between Pt and graphene is considered to be π–d hybridization. Therefore, one can control the electronic structure of graphene and Pt by doping of some elements. In addition, the large surface area of N-G due to it has more sites on which the oxygen binding is very strong. It causes the ORR catalytic activity of N-G is lower than GNS.

Keywords: GNS; N-G; ORR; Pt/GNS.

1. INTRODUCTION

Polymer electrolyte membrane fuel cell (PEMFC) are being developed as electrical power sources for vehicles and portable applications as an alternative to conventional internal combustion engines, secondary batteries, and other conventional power sources [1]. Recently, the design of cheap and stable fuel cell catalysts for ORR is the main challenge [2]. This is caused catalysts exhibit great influence on both the cost and the durability of PEMFC [3]. Platinum (Pt) nano-particles supported on carbon black (Pt/CB) are most used

**Corresponding author: Email: riksonsiburian2000@yahoo.com;*

for ORR catalysts. It has outstanding catalytic and electrical properties [4]. Therefore, much of the art and science of catalysts development for the ORR rely on both the fundamental understanding of the reaction at the Pt electrolyte interface and the optimization of the catalytic properties of the Pt surface [5]. However, Pt is expensive and also it is limited natural resources [6].Therefore, it is a prerequisite to decrease the usage of Pt and enhance the catalytic activity of Pt in order to achieve a competitive low cost of fuel cell.

The catalyst support materials exhibit great influence on the cost, performance, and durability of PEMFC. For instance, carbon-supported precious metal nano-particles (e.g., Pt, Au, Pd, and Rh) are widely used in heterogeneous catalysis and electro catalysis [7]. The support materials are necessary to obtain a high dispersion, narrow distribution of Pt and Pt-alloy nano-particles and also can interplay with catalytic metals, which is the prerequisite to obtain the high catalytic performance of catalysts [1]. Commonly, the catalyst support materials require high specific surface area, high conductivity, low combustive reactivity under both dry and humid air conditions at low temperatures (150ºC or less), high electrochemical stability under fuel cell operating conditions, easy to recover Pt in the used catalyst [1,8], and strong interaction between catalytic metals and the support materials [9]. This is because the interaction between the support and metal catalyst can modify the electronic structure of catalytic metals which in turn changes the catalytic activity [10]. However, the weak interaction between metal and carbon supports results in a severe sintering/agglomeration of catalytic metal nano-particles and consequently decreases the active surface area, which leads to the degradation of performance under long-term operations [7]. Many researchers have reported novel carbon support materials, such as carbon nano-horns [11], carbon nano-coils [12], carbon nano-tube (CNT) [13], graphite nano-fibers (GNFs) [14], and carbon black [15] for PEMFC applications. Some papers also reported that nitrogen-doped carbon nano-tube (N-CNT) with metal catalysts or without metals exhibit enhancement catalytic activity toward ORR [16]. They showed promising results toward fuel cell electrode reactions: ORR and methanol oxidation reaction (MOR). But, in term of activity, cost and durability, current catalysts can still not satisfy the requirements of target PEMFC [17]. Therefore, many efforts are still necessary to find the novel catalytic metals and support materials.

Graphene sheets, a two-dimensional carbon material with single (or a few) atomic layer has attracted great attention for both fundamental science and applied research. This is caused it has large surface area (2630 $m^2 g^{-1}$) [18], and high carrier mobility (104 $cm^2 V^{-1} s^{-1}$ at room temperature) [19]. Recently, graphene as a supporting material for Pt catalyst is believed to improve catalytic activity for hydrogen oxidation reaction (HOR) and methanol oxidation reaction (MOR). However, the controversial results regarding the ORR activity for Pt/GNS compare to platinum on carbon black (Pt/CB) commercial catalyst. Moreover, fuel cell tests with Pt/GNS catalysts as cathode materials showed a considerably lower performance than that of the cell with Pt/CB as cathode catalyst [20].

In this study, I studied the effect of support materials; those are graphene nano-sheets (GNS) and nitrogen doped GNS (N-G) on Pt catalyst for cathode hydrogen fuel cell. In this paper, the ORR catalytic activity of Pt/GNS, Pt/N-G and Pt/CB commercial catalyst as reference were studied, respectively. Because, ORR at the cathode of fuel cells plays a key role in controlling the performance of a fuel cell, and the efficiency of ORR electro-catalysts are essential for fuel cells practical applications [21]. Finally, I expect the support material effect for ORR catalytic activity based on Pt catalyst can be clarified.

2. MATERIALS AND METHODS

2.1 Preparation of Support Materials and Catalysts

In this experiment, two kinds of support materials were prepared, namely graphene nano-sheets (GNS) and nitrogen doped GNS (N-G). Subsequently, Pt atoms were deposited on GNS and N-G, respectively. GNS was prepared by the oxidation of graphite powder using the modified Hummers method [22]. Briefly, graphite powder (0.2 g), particle size 45 µm, (Wako Pure Chemical Industries, Ltd.) and sodium nitrate ($NaNO_3$) (0.16 g) were first stirred in concentrated sulphuric acid (95 wt % H_2SO_4) (6.7 mL) for 2 h while being cooled in an ice water bath. Then, potassium permanganate ($KMnO_4$) (0.9 g) was gradually added to form a new mixture. After 4 h in an ice water bath, the mixture was allowed to stand for 48 h at room temperature with gentle stirring. Thereafter, 20 mL of 5 wt % H_2SO_4 aqueous solution was added into the above mixture over 1 h with stirring. Then, 0.5 mL of H_2O_2 (30 wt % aqueous solution) was also added to the above liquid and the mixture was stirred for 2 h. After that, 20 mL of 3 wt % H_2SO_4/0.5 wt % H_2O_2 solutions was added into suspension and centrifuged (3000 rpm, 1 h). Subsequently, the product was dispersed in water and ultra-sonicated for 5 h. This process affords material of oxidized graphene nano-sheets (OGS) [23]. Finally, the OGS were reduced with hydrazine hydrate at room temperature for 48 h. This product was filtered and washed with distilled water and dried in air at RT for 24 h. The as-received powder is called graphene nano-sheets (GNS). The detail characterization of GNS can be seen in reference as I reported previously [24].

Nitrogen-doped GNS (N-G) was obtained by annealing GNS in pure ammonia (NH_3) (Sumitomo Seika Chemicals) under 0.2 MPa gas flow. The ammonia annealing of GNS was carried out in a homemade tube furnace with connected to gas tanks. Briefly, 100 mg GNS was put into boat glass and placed in the middle of tube furnace. Then, it was annealed by an ammonia stream 50 mL/min at 900ºC for 2h in a furnace, respectively. The powder was collected and denoted as N-doped GNS 900 (N-G). Finally, they were characterized by X-ray photoelectron spectroscopy (XPS) and X-ray diffraction (XRD). In addition, the surface area of carbon black (CB), GNS and N-G was determined by the Brunauer Emmett and Teller (BET) adsorption method are 45, 318 and 594 $m^2 g^{-1}$, respectively. It indicates that in the presence of ammonia on GNS may assist to increase the surface area of N-G. Furthermore, the existence of N atoms in N-G was investigated by XPS measurements.

In order to prepare 20 wt % Pt/GNS, the calculated amount of Pt precursor $H_2PtCl_6 \cdot 6H_2O$ (Alfa Aesar, A Johnson Matthey Company) were dissolved in 50 mL ethanol. Subsequently, each of ethanol solution of the precursor was mixed with ethanol solution of GNS. After stirring solution for 3 h, the product was collected by filtration and dried in air at 60ºC for 12 h. It was then reduced by a hydrogen stream 25 mL/min at 400ºC for 2h in a furnace. Finally, the catalysts were collected and denoted as 20 wt % Pt/GNS.Further, the 20 wt % Pt/N-G catalyst was prepared as same as Pt/GNS catalyst preparation. The amount of Pt on GNS and N-G were measured by thermo-gravimetric/differential thermal analysis (TG/DTA).

Furthermore, the 20 wt % Pt/GNS and Pt/N-G catalysts were characterized by XRD, TEM, XPS, and TG/DTA, respectively. TG/DTA and XRD data can be seen in supporting information (Fig. 1S and 2S). XRD measurements were performed at room temperature employing a two circle diffractometer (PANalytical PW 3050 Philips X'pert Pro, CuK_α radiation of 1.541 Å, without monochromator), installed at a line focus X-ray generator. A reflection free Si plate was used as a sample stage. CuK_α radiation obtained by reflection from singly bent highly oriented pyrolitic graphite (HOPG) crystal was used as the incident X-ray. Diffraction pattern was recorded using a solid state detector (PANalytical X'Celerator)

with a scan speed of 0.05 deg. (in 2θ)/sec up to 90 degrees. XPS measurements were carried out using JEOL JPS 9010 TR (X-ray source AlK_{α}, 1486.6 eV; pass energy 50 eV, energy resolution 1.88 eV which was calibrated using Ag $3d_{5/2}$ by measuring a clean Ag sample, the uncertainty of binding energy ±0.05 eV). TEM (JEOL JEM-1400 electron microscope was operated at 80 kV, resolution lattice image 0.20 nm, and resolution point image 0.38 nm. TG/DTA measurements were carried out using TG/DTA6300, Seiko Instruments Inc. (Reference: Pt; Air 200 mL/min; T measurement: 50–1000ºC; Rate: 10ºC/min), respectively.

2.2 Electrochemical Measurement

The ORR activities of GNS, N-G, 20 wt % Pt/GNS and Pt/N-G catalysts, respectively were assessed by using cyclic voltammetry (CV), and rotating ring disk electrode (RRDE) (PGSTAT PG12, AUTOLAB Potensiostat/Galvanostat) measurements in 0.1 M $HClO_4$. The catalyst ink was prepared by dispersing 1 mg catalyst in the mixture of 500 µL (1:50 in methanol) 5 wt % Nafion solutions (Aldrich), then the mixture of catalyst ink was sonicated for 60 minutes. Then, 10 µL of catalyst ink was transferred onto the polished glassy carbon disk (diameter = 5 mm, geometric area = 0.283 cm^2) and dried to form a thin catalyst layer. The amounts of catalysts loading on the glassy carbon are 20 µg for both GNS and N-G. The rotating ring disk electrode (RRDE) polarization curves of GNS and N-G was obtained in O_2-saturated 0.1 M $HClO_4$ solution.

On the other hand, the Pt loading on the glassy carbon for 20 wt % Pt/GNS, Pt/N-G, and Pt/CB commercial catalysts (Johnson Matthey), respectively was 4 µg. The CV measurement was carried out by using a typical three-electrode systems consist of a working electrode (glassy carbon), a Pt wire as a counter electrode, and a reversible hydrogen electrode (RHE) as a reference electrode. All measurements were performed at room temperature (~25ºC) using a fresh electrolyte solution (0.1 M $HClO_4$, Sigma-Aldrich). First, the catalyst on the working electrode was purged by bubbling nitrogen (N_2) gas at 200 mL min^{-1} through 0.1 M $HClO_4$ for 20 minutes. Then, it was scanned at 0.05–1.0 V versus RHE for 50 cycles with scan rate 10 mVs^{-1} and rotation rate 500 rpm in N_2 to eliminate contaminant and de-oxygenates the environment. After that, the saturation gas was switched to oxygen (O_2) for RRDE measurement, and the electrolyte was saturated for the similar condition as CV measurement. The RRDE polarization curves were obtained at 0.05–1.0 V versus RHE with scan rate 10 mV s^{-1} in O_2 saturated 0.1 M $HClO_4$.

For CO stripping measurements, notice that, the Pt loadings on the working electrode are the same as those measured in ORR. Briefly, each of catalyst ink solutions for 20 wt % Pt/GNS, Pt/N-G, and Pt/CB commercial catalysts, respectively was loaded onto a glassy carbon disk electrode (0.28 cm^2) with diluted (1:50 in methanol) 5 wt % Nafion solution (Aldrich), respectively. Prior to the measurements, the working electrode was firstly purged by bubbling N_2 through the electrolyte solution of 0.1 M $HClO_4$ for 20 minutes, and then it was scanned at - 0.2 to 0.8 V versus Ag/AgCl for 50 cycles in N_2 with scan rate 10 mVs^{-1} and rotation rate 500 rpm for cleaning and de-oxygenates the environment. Subsequently, CO was adsorbed to the surface of the working electrode by bubbling 3 % CO/H_2 into the electrolyte solution of 0.1 M $HClO_4$ at 60ºC for 60 minutes, while holding the working electrode potential at - 0.15 V versus Ag/AgCl. After 3% CO/H_2 bubbling, the gas was switched to N_2 for 30 minutes and the potential was scanned from - 0.2 to 0.8 V versus Ag/AgCl to record the CO stripping voltammogram at 60ºC with a scan rate of 10 mVs^{-1} [25–27]. As a reference, 20 wt % Pt/CB (Alfa Aesar, Johnson Mathew Company) was measured for comparison.

3. RESULTS AND DISCUSSION

3.1 ORR of Pt/GNS, Pt/N-G, and Pt/CB Commercial Catalyst

Fig. 1 shows the ORR activities for 20 wt % Pt/GNS, Pt/N-G, and Pt/CB commercial catalyst.

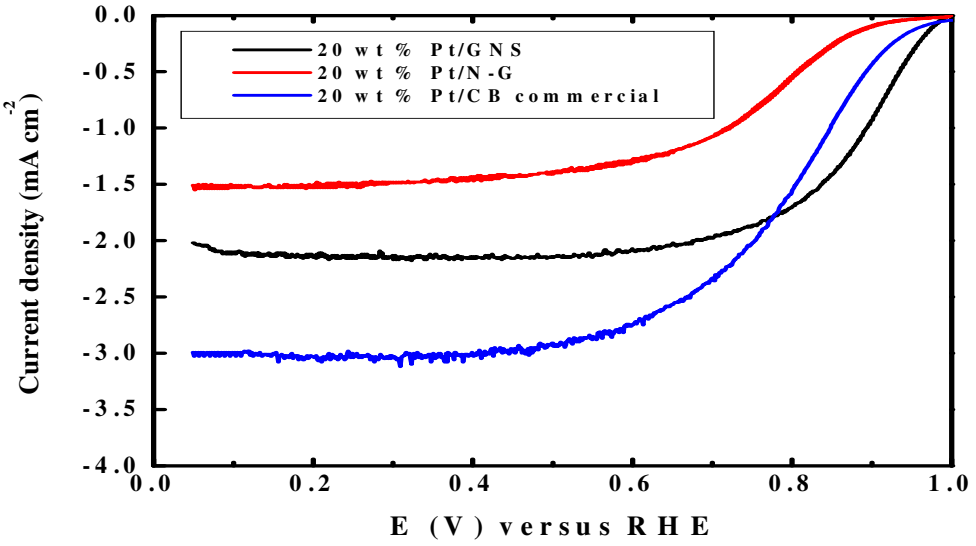

Fig. 1. RRDE polarization curves of 20 wt % Pt/GNS, Pt/N-G, and Pt/CB commercial catalyst in O_2-saturated 0.1 M $HClO_4$ solution. Scan rate is 10 mVs^{-1}. For all the RRDE measurements, the Pt loading of catalysts are 4 µg for 20 wt % Pt/GNS, Pt/N-G, and Pt/CB commercial catalyst, respectively

It clearly shows that the diffusion-limiting currents (below 0.4 V versus RHE) for all the catalysts. However, their diffusion limiting currents are different, depending on support material. This data indicates the catalyst support material affects the diffusion limiting currents values [28]. The ORR activity of Pt/GNS is higher than those of Pt/N-G and Pt/CB commercial catalyst. Further, the Pt/GNS shows the higher ORR activity, corresponding to its onset potential (0.99 V) than Pt/N-G (0.94 V versus RHE). Even the amount of Pt is similar; nevertheless, the ORR activity of catalyst is different. It indicates the Pt electronic structures of each catalyst are different as effect of supporting material. This data is consistent with the results of the current density whereas was measured at 0.9 V versus RHE (Table 1).

Table 1. Current density, average Pt particle size, and BE of Pt 4f for samples

Samples	*j* (0.9 V vs RHE) (mA cm^{-2})	Average Pt particle size (nm) (TEM measurement)	BE of Pt 4f (eV)
20 wt % Pt/GNS	0.9	1.2	71.6
20 wt % Pt/N-G	0.1	1.3	71.7
20 wt % Pt/CB	0.4	2.03	71.4

It clearly shows that the current densities of Pt/GNS, Pt/N-G and Pt/CB are 0.9, 0.1, and 0.4 mA cm^{-2}, respectively. This data also shows that Pt/GNS is higher ORR activity than Pt/N-G.

It is caused the support material effect. For the ORR, the too high reactivity of the support material impedes reaction by blocking the active sites with strong oxygen binding, while too low reactivity hinders the dissociation of O–O bond and charge transfer [29].

3.2 TEM

The TEM images and histograms of 20 wt % Pt/GNS, Pt/N-GNS, and Pt/CB commercial catalysts are shown in Fig. 2.

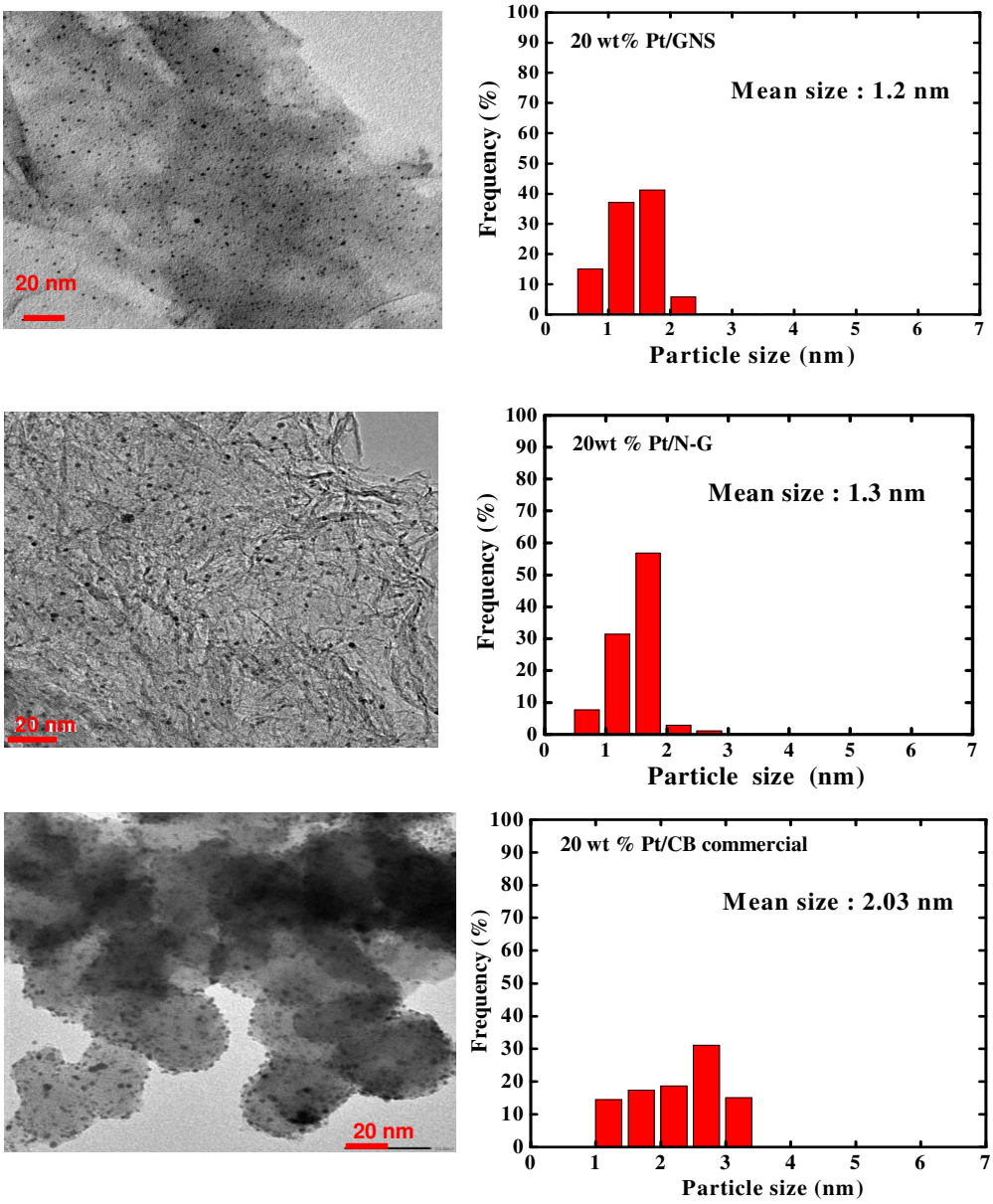

Fig. 2. TEM images and histograms of 20 wt % Pt/GNS, Pt/N-G, and Pt/CB commercial catalyst, respectively

The Pt particle size distributions were analyzed with random chosen areas containing 600 particles in magnified TEM images. The Pt particle size only was estimated base on Pt particles (< 5 nm). As shown in TEM images, the Pt particles are good dispersing on GNS, N-G, and CB. The average Pt particle size of Pt/GNS, Pt/N-G, and Pt/CB are 1.2, 1.3, and 2.03 nm, respectively (Table 1). Interestingly, the Pt diameters less than 1 nm (Pt subnano-clusters) were only formed on GNS and N-G, but not on CB. It means the GNS and N-G as supporting materials may play important role on formation of Pt subnano-clusters. The Pt subnano-clusters are much more formed on Pt/GNS than that of Pt/N-G. As shown in Table 1, the ORR activity of Pt/GNS is higher than Pt/N-G. I suppose there are two factors which affect it namely the support material effect and Pt subnano-clusters. At the same amount (20 wt % Pt), Pt supported on GNS has the highest ORR catalytic activity among Pt/N-G and Pt/CB. It is caused the support material effect. In addition, in term of Pt/CB, there is no Pt subnano clusters are formed. On the other hand, Pt subnano clusters are formed on GNS and N-G. It is responsible causing the ORR catalytic activity of Pt/GNS and Pt/N-G is higher than Pt/CB.

3.3 XPS

Fig. 3 shows the Pt 4f XPS spectra for 20 wt % Pt/GNS, Pt/N-G, and Pt/CB commercial catalyst.

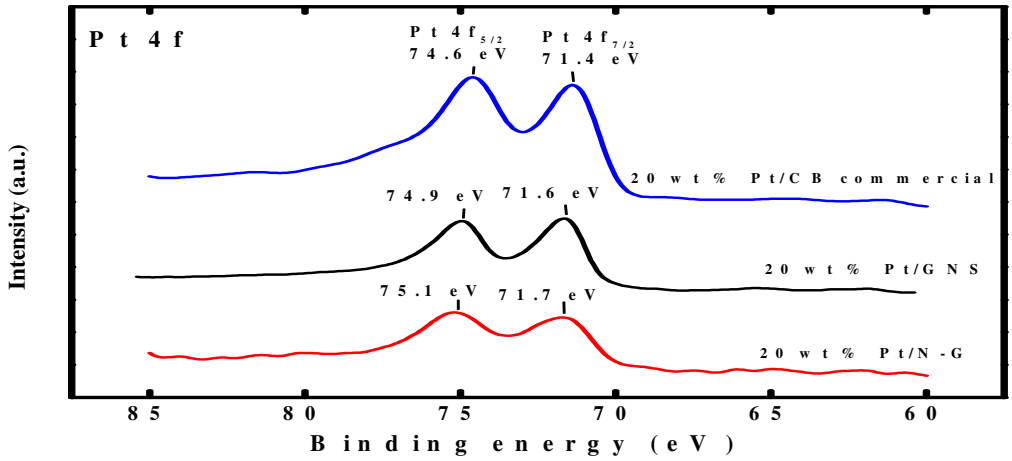

Fig. 3. XPS spectra for 20 wt % Pt/GNS, Pt/N-G, and Pt/CB commercial catalyst

The binding energies (BEs) are 71.6, 71.7, and 71.4 eV for Pt/GNS, Pt/N-G, and Pt/CB, respectively (Table 1). The BE of Pt on Pt/CB is close to the bulk Pt (71.2 eV) [30], indicating the weak interaction between Pt and CB. Interestingly, the BEs of Pt on Pt/GNS and Pt/N-G shift to higher binding energy compare to Pt/CB. It indicates that GNS and N-G significantly influence the π–d interaction in terms of Pt electronic structure. Therefore, the GNS and N-G can be expected to modify the Pt electronic structure. XPS data (Fig. 3) shows that interaction between Pt and CB is normally Pt because binding energy of Pt does not shift to higher binding energy. It means interaction between Pt and CB is weak. It is not good catalyst due to support material can release during extent use and also Pt can be blocked by the other compound. In contrast, the binding energy of Pt/GNS and Pt/N-G shift to higher binding energy, indicating strong interaction between Pt and graphene. It is possible due to

graphene and Pt has π-conjugated and d-orbital, respectively. Thereby, Pt electronic states are modulated on GNS due to π-d hybridization. This is also the reason why the ORR activity of Pt/GNS is highest among the others, because the strong interaction between Pt and GNS, probably π–d interaction. In addition, there are three possibilities nitrogen species doped in graphene layer, namely pyridine, graphitic and amino types. It suggests that the graphene sheets in N-G have fewer atomic layers than GNS. It also indicates that the increasing surface area is associated with more edge sites. The large surface area of N-G causes the strong interaction between oxygen and carbon [29], resulting a low ORR activity.

Therefore, the Pt subnano-clusters and graphene are responsible for causing high ORR catalytic activity of Pt/GNS. I consider two factors, those are i) Enthalpy factor ascribes the interface interaction Pt**-**C via the π-d hybridization. It is possible due to the reactivity of graphene's π-conjugated states, and ii) Entropy factor. GNS has large surface area. It is required for high dispersion of small Pt particles.

4. CONCLUSION

In this study, the GNS and N-G were used as supporting materials to deposit Pt particles in order to investigate the support material effect for ORR activity. The ORR activity of Pt/GNS is higher than Pt/N-G catalysts. This suggests that the modification of π states by the N-doping change the properties of the interaction between Pt and carbon. The interaction between Pt and graphene is considered to be π–d hybridization. Therefore, one can control the electronic structure of graphene and Pt by doping of some elements. On the other hand, since the particle sizes and binding energies are similar and the surface areas are different, the difference between GNS and N-G is related to surface area. The greater surface area has more sites on which the oxygen binding is very strong. It also causes the ORR catalytic activity of Pt/N-G is lower than Pt/GNS.

COMPETING INTERESTS

Author has declared that no competing interests exist.

REFERENCES

1. Shao Y, Liu J, Wang Y, Lin Y. Novel Catalyst Support Materials for PEM Fuel Cells: Current Status and Future Prospects. J Mat Chem. 2009;19(1):46-59.
2. Gasteiger HA, Markovic NM. Just a Dream or Future Reality. Science. 2009;324(5923):48-49.
3. Gasteiger HA, Kocha SS, Sompalli B, Wagner TF. Activity benchmarks and requirements for Pt, Pt-alloy, and non-Pt oxygen reduction catalysts for PEMFCs. Appl Catal B Environ. 2005;56(1-2):9-35.
4. Peng Z, Yang H. Designer platinum nanoparticles: Control of shape, composition in alloy, nanostructure and electrocatalytic property. Nano Today. 2009;4(2):143-164.
5. Markovic NM, Schmidt TJ, Stamenkovic V, Ross PN. Oxygen Reduction Reaction on Pt and Pt Bimetallic Surfaces: A Selective Review. Fuel Cells. 2001;1(2):105-116.
6. Berger DJ. Fuel Cells and Precious-Metal Catalysts. Science. 1999;286(5437):49-50.
7. Kou R, Shao Y, Mei D, Nie Z, Wang D, Wang C, Viswanathan VV, Park S, Aksay IA, Lin Y, Wang Y, Liu J. Stabilization of electrocatalytic metal nanoparticles at metal-metal oxide-graphene triple junction points. J Am Chem Soc. 2011;133(8):2541-2547.

8. Shao Y, Yin G, Gao Y. Understanding and approaches for the durability issues of Pt-based catalysts for PEM fuel cell. J Power Sources. 2007;171(2):558-566.
9. Zhou JG, Zhou XT, Sun XH, Li RY, Murphy M, Ding ZF, Sun XL, Sham TK. Interaction between Pt nanoparticles and carbon nanotubes-An X-ray absorption near edge structures (XANES) study. Chem Phys Lett. 2007;437(4-6):229-232.
10. Shao Y, Sui J, Yin G, Gao Y. Nitrogen-doped carbon nanostructures and their composites as catalytic materials for proton exchange membrane fuel cell. Appl Catal B. 2008;79(1):89-99.
11. Yoshitake T, Shimakawa Y, Kuroshima S, Kimura H, Ichihashi T, Kubo Y, Kasuya D, Takahashi K, Kokai F, Yudasaka M, Iijima S. Preparation of fine platinum catalyst supported on single-wall carbon nanohorns. Physica B. 2002;323(1-4):124-126.
12. Park KW, Sung YE, Han S, Yun Y, Hyeon T. Origin of the Enhanced Catalytic Activity of Carbon Nanocoil-Supported PtRu Alloy Electrocatalysts. J Phys Chem B. 2004;108(3):939-944.
13. Shao YY, Yin GP, Wang JJ, Gao YZ, Shi PF. Multi-walled carbon nanotubes based Pt electrodes prepared with in situ ion exchange method for oxygen reduction. J Power Sources. 2006;161(1):47-53.
14. Bessel CA, Laubernds K, Rodriguez NM, Baker RTK. Graphite nanofibers as an electrode for fuel cell applications. J Phys Chem B. 2001;105(6):1115-1118.
15. Wang J, Yin G, Shao Y, Zhang S, Wang Z, Gao Y. Effect of carbon black support corrosion on the durability of Pt/C catalyst. J Power Sources. 2007;171(2):331-339.
16. Sun CL, Chen LC, Su MC, Hong LS, Chyan O, Hsu CY, Chen KH, Chang TF, Chang L. Ultrafine platinum nanoparticles uniformly dispersed on arrayed CNx nanotubes with high electrochemical activity. Chem Mater. 2005;17(14):3749-3753.
17. Shao YY, Yin GP, Wang ZB, Gao YZ. Proton exchange membrane fuel cell from low temperature to high temperature: Material challenges. J Power Sources. 2007;167(2):235-242.
18. Stoller MD, Park S, Zhu Y, An J, Ruoff RS. Graphene-Based Ultracapacitors. Nano Lett. 2008;8(10):3498-3502.
19. Novoselov KS, Geim A, Morozov SV, Jiang D, Zhang Y, Dubonos SV, Grigorieva IV, Firsov AA. Electric Field Effect in Atomically Thin Carbon Films. Science. 2004;306(5696): 666-669.
20. Antolini E. Graphene as a new carbon support for low-temperature fuel cell catalysts. Applied Catalysis B Environmental. 2012;123-124:52-68.
21. Cherstiouk OV, Simonov PA, Savinova ER. Model approach to evaluate particle size effects in electrocatalysis: preparation and properties of Pt nanoparticles supported on GC and HOPG. Electrochim Acta. 2003;48(25-26):3851-3860.
22. Hummers WS, Offeman RE. Preparation of Graphitic Oxide. J Am Chem Soc. 1958;80(6):1339-1339.
23. Stankovich S, Dikin DA, Dommett GHB, Kohlhaas KM, Zimney EJ, Stach EA, Piner RD, Nguyen ST, Ruoff RS. Graphene-based composite materials. Nature. 2006;442:282-286.
24. Siburian R, Nakamura J. Formation Process of Pt Subnano-Clusters on Graphene. J Phys Chem C. 2012;116(43):22947-22953.
25. Joo JB, Kim P, Kim W, Kim Y, Yi J. Effect of the preparation conditions of carbon-supported Pt catalyst on PEMFC performance. J Appl Electrochem. 2009;39(1):135-140.
26. Vidakovic T, Christov M, Sundmacher K. The use of CO stripping for in situ fuel cell catalyst characterization. Electrochim Acta. 2007;52(18):5606-5613.

27. Cherstiouk OV, Simonov PA, Savinova ER. Model approach to evaluate particle size effects in electrocatalysis: preparation and properties of Pt nanoparticles supported on GC and HOPG. Electrochim Acta. 2003;48(28):3851-3860.
28. He D, Cheng K, Li H, Peng T, Xu F, Mu S, Pan M. Highly active platinum nonoparticles on graphene nanosheets with a Significant Improvement in Stability and CO Tolerance. Langmuir. 2012;28(8):3979-3986.
29. Shao M, Peles A, Shoemaker K. Electrocatalysis on Platinum Nanoparticles: Particle Size Effect on Oxygen Reduction Reaction Activity. Nano Lett. 2011;11(9):3714-3719.
30. Moulder J, Stickle WF, Sobol PE, Bomben KD. Handbook of X-ray Photoelectron Spectroscopy, 2nd ed. Perkin Elmer Corporation: Minnesota USA; 1992.

Peer-review history:
The peer review history for this paper can be accessed here:
http://www.sciencedomain.org/review-history.php?iid=500&id=7&aid=4572